Symbolic Dynamics for the Hénon–Heiles Hamiltonian on the Critical Level[1]

Gianni Arioli

Dip. di Scienze e T.A., *C.so Borsalino 54*, *15100 Alessandria, Italy*
E-mail: gianni@mfn.al.unipmn.it

and

Piotr Zgliczyński[2]

School of Mathematics, *Georgia Institute of Technology*,

We present a computer assisted proof of the existence of a rich symbolic dynamic structure for the Hénon–Heiles Hamiltonian system at the critical energy $E = 1/6$.
© 2001 Academic Press

Key Words: symbolic dynamics; periodic points; covering relations; computer assisted proof.

1. INTRODUCTION

We investigate the Hénon–Heiles system introduced in [HH], defined by the Hamiltonian

$$H = \frac{p_x^2 + p_y^2}{2} + \frac{x^2 + y^2}{2} + x^2 y - \frac{y^3}{3}. \tag{1.1}$$

The corresponding Hamilton equations are:

$$\begin{aligned}
\dot{p}_x &= -x - 2xy \\
\dot{p}_y &= -x^2 + y^2 - y \\
\dot{x} &= p_x \\
\dot{y} &= p_y
\end{aligned} \tag{1.2}$$

The system is autonomous; therefore an integral of motion is provided by the energy H. In other words, the energy levels $\{(x, y, p_x, p_y) \in \mathbb{R}^4 : H(p_x, p_y, x, y) = h\}$, denoted by $H = h$, are invariant under the flow generated by (1.2). The interest in the Hénon–Heiles system was initially motivated by the search for additional conservation laws in certain galactic potentials admitting an axis of symmetry; Hénon and Heiles presented the Hamiltonian (1.1) as a model problem. Later it was observed in [LF] that a wide class of three particle systems can be reduced to a Hénon–Heiles-type Hamiltonian by considering only the first three terms in the Taylor expansion (see also [BGM] for a list of problems related to this model).

The numerical simulations of the Poincaré return map of system (1.2) at the section $x = 0$, $\dot{x} > 0$ performed by Hénon and Heiles [HH] show an interesting dynamical behavior for the energy range $0 < h \leqslant 1/6$. When h is small the system appears to be integrable, with large elliptic islands dominating the picture of the dynamics. Then, as the energy increases, some small chaotic regions arise, which tend to grow at the expense of the elliptic islands. Finally, at $h = 1/6$ the chaotic regions dominate the whole picture, with apparently only two small elliptic islands left.

Much of the research on the Hénon–Heiles system aimed at explaining this striking behavior was done in the 1970s; see the survey paper by Churchill, Pecelli, and Rod [CPR] and also [CKR]. We describe briefly the results of this development. In the following the names for the main families of periodic orbits are those used in [CPR]. We do not pursue the issue of integrability of the Hénon–Heiles system here; the interested reader is referred to [MC, MP] and references given there.

When $h < 0$ the dynamics of the Hénon–Heiles system is rather uninteresting, since all solutions escape to infinity in both time directions. When $h = 0$ a critical point appears at the origin, and as h becomes positive eight main families of periodic orbits Π_i, $i = 1, ..., 8$, arise. All these periodic orbits lie on a compact component of the manifold $H = h$ and exist in the whole energy range $0 < h < \frac{1}{6}$. At $h = \frac{1}{6}$ three new symmetrically placed critical points appear, each bifurcating into a hyperbolic periodic orbit when $h > \frac{1}{6}$. We call those orbits P_i, $i = 1, 2, 3$. At energy $h = \frac{1}{6}$ the periodic orbits Π_i, $i = 1, 2, 3$, degenerate into orbits homoclinic to the newborn critical points and they disappear for higher energies. The remaining orbits

Π_i, $i = 4, ..., 8$, continue to exist at least for energies $h < \frac{1}{6} + \delta$, for some $\delta > 0$. It also known (see [CPRI]) that the stability type of the orbits Π_i, $i = 1, 2, 3$ changes infinitely many times from hyperbolic to elliptic and vice versa as $h \uparrow \frac{1}{6}$. The stability type of Π_i, $i = 4, 5, 6$ is believed to be hyperbolic and the orbits Π_i, $i = 7, 8$ are believed to be elliptic for small h and then hyperbolic near $h = \frac{1}{6}$. In [CRIV] the existence of heteroclinic orbits between Π_4, Π_5, and Π_6 was established for sufficiently small $h > 0$.

Obviously the above listing of main families, periodic solutions does not solve the question of the existence of some stochastic behavior for the Hénon–Heiles system. All rigorous results concerning chaotic behavior for (1.2) are obtained for energies $h > \frac{1}{6}$. Churchill and Rod (see [CRIII]) have shown that for sufficiently high energy $h > \frac{1}{6}$ and for $i = 1, 2, 3$ the stable manifold of P_i and the unstable manifolds of P_j, $j \neq i$, intersect transversally, giving rise to multiple Smale's horseshoes.

In the papers [GR1, GR2, L, MHO] a different approach was used to prove some chaotic behavior for energies $\frac{1}{6} < h < \frac{1}{6} + \delta$ for some small $\delta > 0$. This approach is based on the existence for $h = \frac{1}{6}$ of an orbit homoclinic to a critical saddle–center point. In fact, we have three homoclinic orbits Γ_i for $i = 1, 2, 3$ (these are the limits of the orbits Π_i as $h \uparrow \frac{1}{6}$; see Section 3 for more details). It is possible then to derive an asymptotic expression for the Poincaré map F_i on the section $y = 0$, $\dot{y} > 0$ for points which remain close to Γ_i at all times. From this asymptotic expression it was shown that the maps F_i admit hyperbolic sets with horseshoe dynamics near Γ_i for $\frac{1}{6} < h < \frac{1}{6} + \delta$.

In this paper we prove that the Hénon–Heiles system embeds a rich symbolic dynamic structure and it has an infinite number of periodic points for energies in the range $h \in (\frac{1}{6} - \delta, \frac{1}{6} + \delta)$ for some $\delta > 0$. We investigate the Poincaré map defined on the section $x = 0$, $\dot{x} > 0$, which is the same section considered in [HH]. Roughly speaking, we show the following: there exists an invariant set S which contains the orbits Π_i, $i = 4, 5, 6$. On the set S we prove the existence of the same symbolic dynamics we would get if we knew that the stable manifolds of Π_i intersected the unstable manifolds of Π_j for $i, j = 4, 5, 6$. On the other hand, we did not prove the hyperbolicity of S. We remark that, even for $h > \frac{1}{6}$, our result is not contained in the papers mentioned above; indeed we explore a different region of the phase space, far away from the homoclinic orbit. For a detailed description of the results we refer the reader to Section 5.

In order to prove the existence of symbolic dynamics, we use the topological method developed in [Z1, Z2, GZ]. The basic tools in this method are the covering relations and the fixed point index. See Section 4 for a detailed exposition of the method.

A basic feature of our procedure is that we do not have any assumption involving derivatives. In fact, this method has a lot in common with the

classical approach used for dealing with Smale's horseshoes (see for example [GH]). From the assumptions used there, we drop all those involving derivatives (cone conditions). We keep the assumptions concerning how the image of some sets is located with respect to other sets, which is precisely our definition of the covering relation. By this method, given an approximate transversal intersection of the stable and unstable manifolds, we are able to explicitly build the sets on which the symbolic dynamics is obtained, but we do not need to verify what is the relation between our approximate invariant manifolds and the true invariant manifolds. This is the reason that makes the method applicable.

We want to point out that purely topological methods in the context of the Henon–Heiles hamiltonian were introduced in the papers by Churchill and Rod [CRI, CRII] (see also [E]). The method presented here appears to be both more elementary and more general.

Another important feature of our proof is that we check all covering relations with computer assistance, i.e., we do rigorous numerics. Since our method is purely topological (i.e., it only involves C^0 assumptions), we were able to perform all necessary numerics in a reasonable time (about 2 hours and 40 minutes on a Pentium III computer).

We conclude with some remarks on computer assisted proofs of chaotic behavior for dynamical systems. At this moment there exists a number of such proofs. The reason to use computers is our inability to solve the equations in regions far from some special orbits, even with a suitable approximation.

Some of the existing computer assisted proofs exploit special properties of the system under consideration. This is the case for the first rigorous proof of existence of chaotic solutions for the Lorenz system in [HZHT]. Also, the recent proof of the existence of the Lorenz attractor by Tucker [T] is devised especially for this particular system, but obviously the result is very strong in that case, as he is able to prove that the dynamics on the whole Lorenz attractor is hyperbolic.

Other methods used in computer assisted proofs are more general, in fact they do not depend upon the particular system under consideration. One such method (see [NR, RNS]) is to show rigorously the transversality of the intersection of stable and unstable manifolds of fixed points or periodic orbits. To apply this method we need rigorous algorithms to build the stable and unstable manifolds. This is done in [NR, RNS] for one-dimensional stable and unstable manifolds. This requires some rigorous C^1 computations. This method does not give any information about the lower bound for the topological entropy of the map under consideration or about the periods of the periodic points.

The proof we present here and the proofs in [MM2, MM3, Z2, GZ] are examples of applications of topological methods in chaotic dynamics.

These methods do not depend upon C^1-details of the system under consideration, but only require some C^0-information on the Poincaré map as an input to compute topological invariants, like the Conley index or the fixed point index. The fact that we need to perform only C^0 computations is very important and results in much shorter computation times when compared to methods requiring C^1 estimates. Obviously this is a strong side of these methods, but there is also a weak side, since all the information concerning C^1 properties like the hyperbolicity of the invariant set is not available.

The layout of the paper is as follows: In Section 2 we discuss some properties of the system and we describe the idea underlying the proof of the results. In Section 3 we discuss the Poincaré return map. In Section 4 we describe the topological methods we use. In Section 5 we give all the results we obtain, and in the last section we provide a description of the numerics involved.

2. DESCRIPTION OF THE SYSTEM

System (1.2) is invariant under the symmetries given by the time reversal, the maps $(p_x, x) \mapsto (-p_x, -x)$ and $(x, y, p_x, p_y) \mapsto R_\pm(x, y, p_x, p_y)$, where the matrices $R_\pm$ are defined by

$$\begin{bmatrix} \cos\left(\pm\frac{2\pi}{3}\right) & -\sin\left(\pm\frac{2\pi}{3}\right) & 0 & 0 \\ \sin\left(\pm\frac{2\pi}{3}\right) & \cos\left(\pm\frac{2\pi}{3}\right) & 0 & 0 \\ 0 & 0 & \cos\left(\pm\frac{2\pi}{3}\right) & -\sin\left(\pm\frac{2\pi}{3}\right) \\ 0 & 0 & \sin\left(\pm\frac{2\pi}{3}\right) & \cos\left(\pm\frac{2\pi}{3}\right) \end{bmatrix}.$$

Consider the Poincaré section Θ_1 defined by $H = 1/6$, $x = 0$, $\dot{x} > 0$; in fact from now on we denote by Θ_1 the projection of the Poincaré section on the plane (y, p_y) and we use the coordinates (y, p_y) to denote points on Θ_1. Let Θ_2 and Θ_3 be the Poincaré sections obtained by the symmetries $R_\pm$ from Θ_1. More precisely, we define $\Theta_2 = R_-(\Theta_1)$ and $\Theta_3 = R_+(\Theta_1)$. Finally let $\Theta = \bigcup_i \Theta_i$.

Let $P_1 : \mathrm{dom}(P_1) \subset \Theta_1 \to \Theta_1$ be the Poincaré map (the actual domain of the map is described in Section 3).

In this paper we focus on the periodic orbits Π_i, $i = 4, 5, 6$. Following [CPR] we call Π_i both the periodic orbits and their intersection with Θ_1,

which are fixed points for the Poincaré map. Note that the orbit Π_4 intersects Θ_1 in a point ($x = 0$, $y < 0$, $p_x > 0$, $p_y = 0$) (see Fig. 2 in [CPR] and apply transformation $(x, y) \mapsto -(y, x)$). The other orbits are $\Pi_5 = R_-(\Pi_4)$ and $\Pi_6 = R_+(\Pi_4)$; it follows from the geometrical construction of these orbits in [CPR] that the intersection of each of these orbits with Θ_1 consists in just one point and we have $\Pi_5 = (\bar{y}, p_y^-)$ and $\Pi_6 = (\bar{y}, -p_y^-) = M(\Pi_5)$ for some $\bar{y}$ and $p_y^- > 0$. It can be observed numerically that P_1 has a fixed point in a neighborhood of $(-1/4, 0)$ (and the existence of such fixed point is rigorously proved as a byproduct of our result). We identify this point with Π_4. The periodic orbits Π_5 and Π_6, obtained by the symmetry given by $R_\pm$ from Π_4, also intersect Θ_1 at two other fixed points of the map P_1 (see Fig. 1). We have $\Pi_5 \simeq (0.37, 0.30)$ and $\Pi_6 \simeq (0.37, -0.30)$.

If $x \in \Theta_1$ is a fixed point for the Poincaré map, by $W_s(x)$ ($W_u(x)$) we denote its stable (unstable) manifold. Finally let M be the map corresponding to the symmetry about the y axis, i.e., $M(y, p_y) = (y, -p_y)$.

2.1. Approximate Stable and Unstable Manifolds for Π_4, Π_5, Π_6

Figure 1 displays the computer-generated approximate stable and unstable invariant manifolds for the points Π_i. The black branches are the unstable manifolds (denoted by u) and the grey branches are the stable manifolds (denoted by s). The rule for naming various branches is the following: for Π_4, which is located on the line $y = 0$, we denote the branch of invariant manifolds which enter into the upper half-plane with the subscript 1, those entering the lower part have the subscript 2. For invariant manifolds of Π_5 we use primes and for those of Π_6 we use double primes.
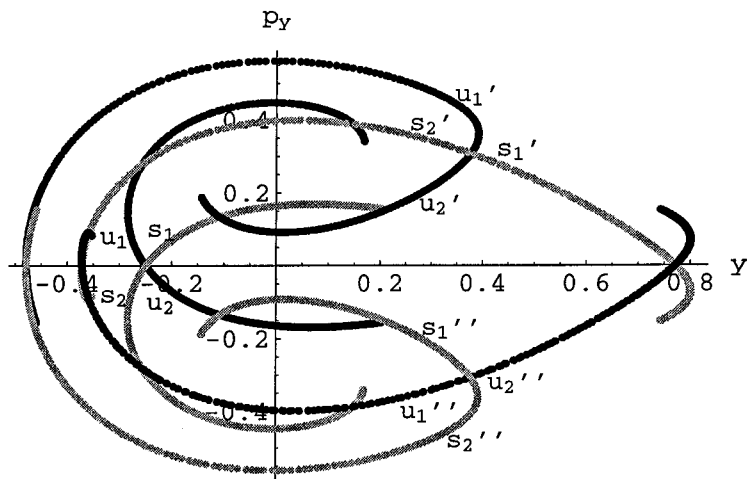

FIG. 1. Approximate stable and unstable manifolds of Π_i, $i = 4, 5, 6$.

The subscripts 1 and 2 are assigned to various branches by symmetry: $u'_j = R_- u_j$, $s'_j = R_- u_j$, $u''_j = R_+ u_j$, $s''_j = R_+ u_j$ for $j = 1, 2$.

Observe that the rotational symmetries of the system R_- and R_+ are not explicit in Fig. 1. This is due to the fact that the Poincaré section Θ_1 is not invariant with respect to R_- and R_+. One can try to recover those symmetries as non-linear maps which are a composition of the rotation R_- (R_+) and the Poincaré map between sections Θ_1 and $R_- \Theta_1$ ($R_+ \Theta$), but since these maps are not given explicitly, we do not pursue this attempt any further. Instead, we exploit the symmetries R_- and R_+ by noting that the Poincaré maps on Θ_2 and Θ_3 are conjugated to the Poincaré map on Θ_1 by these rotations.

The symmetry of this picture with respect to the reflection about the line $y = 0$ (the map M) is a consequence of the symmetries of the Hénon–Heiles equations, as is explained by the following lemma.

LEMMA 1. *If $P(y, p_y) = (\tilde{y}, \tilde{p}_y)$, then $P(\tilde{y}, -\tilde{p}_y) = (y, -p_y)$. Furthermore, $(y, p_y) \in W_s(\Pi_i)$ if and only if $(y, -p_y) \in W_u(M(\Pi_i))$.*

Proof. Let h be the energy. Let $p_x(y, p_y)$ be the value of p_x for a point on Θ_1,

$$p_x(y, p_y) = \sqrt{2h - p_y^2 - y^2 + y^3/3}.$$

Let $\varphi: \mathbb{R} \times \mathbb{R}^4 \to \mathbb{R}^4$ be the dynamical system defined by (1.2); in other words the function $t \mapsto \varphi(t, (x_0, y_0, p_{x0}, p_{y0}))$ is a solution to the system (1.2) with initial conditions at time $t_0 = 0$ set to $(x_0, y_0, p_{x0}, p_{y0})$. By φ_x we denote the x-component of φ.

By the definition of a Poincaré map, $P(y, p_y) = (\tilde{y}, \tilde{p}_y)$ means that there exists a $T > 0$ such that

$$\varphi(T, (0, y, p_x(y, p_y), p_y)) = (0, \tilde{y}, p_x(\tilde{y}, \tilde{p}_y), \tilde{p}_y), \tag{2.1}$$

and for all $0 < t < T$, either,

$$\varphi_x(t, (0, y, p_x(y, p_y), p_y)) \neq 0$$

or

$$\frac{d}{dt} \varphi_x(t, (0, y, p_x(y, p_y), p_y)) < 0. \tag{2.2}$$

After applying the time reversal symmetry to (2.1)–(2.2) we obtain

$$\varphi(T, (0, \tilde{y}, -p_x(\tilde{y}, \tilde{p}_y), -\tilde{p}_y)) = (0, y, -p_x(y, p_y), -p_y) \tag{2.3}$$

and, for $0 < t < T$, either

$$\varphi_x(t, (0, \tilde{y}, -p_x(\tilde{y}, \tilde{p}_y), -\tilde{p}_y)) \neq 0$$

or

$$\frac{d}{dt} \varphi_x(t, (0, \tilde{y}, -p_x(\tilde{y}, \tilde{p}_y), -\tilde{p}_y)) > 0. \tag{2.4}$$

The reflection against the y axis $(x, p_x) \to (-x, -p_x)$ transforms conditions (2.3)–(2.4) into

$$\varphi(T, (0, \tilde{y}, p_x(\tilde{y}, \tilde{p}_y), -\tilde{p}_y)) = (0, y, p_x(y, p_y), -p_y) \tag{2.5}$$

and, for $0 < t < T$, either

$$\varphi_x(t, (0, \tilde{y}, p_x(\tilde{y}, \tilde{p}_y), -\tilde{p}_y)) \neq 0$$

or

$$\frac{d}{dt} \varphi_x(t, (0, \tilde{y}, p_x(\tilde{y}, \tilde{p}_y), -\tilde{p}_y)) < 0. \tag{2.6}$$

Since $p_x(y, -p_y) = p_x(y, p_y)$, the conditions (2.5)–(2.6) are equivalent to

$$P(\tilde{y}, -\tilde{p}_y) = (y, -p_y);$$

hence we have proved the first assertion of the lemma. The second one follows easily. ∎

Observe that Fig. 1. strongly suggests that the fixed points Π_i, $i = 4, 5, 6$, are hyperbolic and that we have following transversal intersections:

$$u_1 \pitchfork s_2', u_1' \pitchfork s_2'', u_1'' \pitchfork s_2$$
$$u_2 \pitchfork s_1'', u_2'' \pitchfork s_1', u_2' \pitchfork s_1.$$

Now using the standard argument from the proof of the Smale–Birkhoff homoclinic theorem (see Theorem 5.3.5 in [GH]) one can argue that for some iteration of the Poincaré map P we have a hyperbolic invariant set containing Π_i, $i = 4, 5, 6$ and the symbolic dynamics contains the following transitions:

$$M_4 \to M_4, M_5, M_6 \qquad M_5 \to M_4, M_5, M_6, \qquad M_6 \to M_4, M_5, M_6,$$

where M_i are some tiny sets such that $\Pi_i \in M_i$. In the next subsection we repeat an essential part of this argument in the description of our method

of exploiting the apparent transversal intersections of the invariant manifolds to obtain some symbolic dynamics.

2.2. *The Construction of the Sets*

We follow the standard argument mentioned above to construct the sets M_i explicitly. To this aim we have to use auxiliary sets, which are located on the intersections of stable and unstable manifolds under consideration. In our approach we do not need any information about hyperbolicity, hence we neither have to worry about rigorous linearization of the Poincaré map around the points Π_i, nor do we have to perform the analysis involved in the λ-lemma (see Theorem 5.2.10 in [GH]).

As an example we describe how we exploit the apparent transversal intersections

$$u_1 \pitchfork s_2', \qquad u_2' \pitchfork s_1, \qquad (2.7)$$

to build symbolic dynamics on two symbols in the neighborhood of Π_4.

In this construction we use the covering relation $\Rightarrow$ which is precisely defined in Section 4; here we only present a heuristic description.

We consider parallelograms on the plane. For each parallelogram we choose an expanding direction and a contracting direction (these are just names, we do not rigorously check if we actually have expansion or contraction). As a rule, the expanding direction is along the unstable manifold under consideration. The relation $M \overset{P}{\Rightarrow} N$ means that M is mapped across N in the expanding direction and $P(M)$ do not intersect the edges of N which are parallel to the expanding direction (see Fig. 5).

In this construction we place all parallelograms along either u_1 or u_2'.

1a: Close to Π_4.   We start with a set M_0 such that $\Pi_4 \in M_0$, M_0 is oriented along u_1 and satisfies $M_0 \overset{P}{\Rightarrow} M_0$.

1b: Close to Π_5.   We construct M_0' with the same criterion as in 1a.

2a: Reaching $u_1 \cap s_2'$ from M_0.   We need to find sets M_1, M_2, ..., M_{k_1} such that $M_i \overset{P}{\Rightarrow} M_{i+1}$ for $i = 0, ..., k-1$ and the last set in this sequence is such that the intersection of u_1 and s_2' is located in the interior of M_k and s_2' intersects M_k transversally in the expanding direction (which is close to that of u_1). Observe that this is possible due to apparent transversal intersection of $u_1 \cap c_2'$. In our case we have $k_1 = 2$.

2b: Reaching $u_2' \cap s_1$ from M_0'.   As in step 2a.

3a: Getting close to Π_5 and u' from M_{k_1}.   Since M_k is located across s_2', then the iterates of M_k bring M_k close to $u' = u_1' \cup u_2'$. There is also

expansion along u'. Hence we can find a sequence $M_{k_1}, ..., M_{k_2}$, such that

$$M_{k_1} \overset{P}{\Rightarrow} M_{k_1+1} \overset{P}{\Rightarrow} \cdots \overset{P}{\Rightarrow} \cdots M_{k_2} \overset{P}{\Rightarrow} M'_0 \cup M'_1 .$$

In our case $k_2 = k_1$.

   3b: Getting close to Π_4 and u from M'_{k_1}. As in step 3a.

   4: Closing the loop. Observe that as a results of the previous steps we get

$$M_0 \overset{P}{\Rightarrow} M_0, M_1$$

and

$$M_1 \overset{P}{\Rightarrow} M_2 \overset{P}{\Rightarrow} \cdots \overset{P}{\Rightarrow} M_{k_2} \overset{P}{\Rightarrow} M'_1 \overset{P}{\Rightarrow} \cdots \overset{P}{\Rightarrow} M'_{k'_2} \overset{P}{\Rightarrow} M_0, M_1.$$

We have built transitions from M_n to M_l, $l, m = 0, 1$, using covering relations. These transitions yield (see Section 4) the existence of symbolic dynamics on two symbols for $P^{k_2+k'_2}$, with periodic points corresponding to periodic sequences.

   This is the idea of the procedure we used to build the sets M_j, $j = 0, 4$, which are used in the actual proof.

   Figure 6 shows the sets M_j (and some other sets N_j which will be introduced in the sequel) and the location of the invariant manifolds for Π_4 and Π_5.

2.3. Comparison with the Standard Argument

   The standard argument [GH] applied to (2.7) goes essentially through the same steps described above. The essential difference is in the size of sets M_i and their number.

   Let U_4 and U_5 be neighborhoods of Π_4 and Π_5, such that the behavior of $P_{|U_i}$ is hyperbolic. To give (or compute) a lower bound for the size of U_i is a rather hard task (even with computer assistance). As a result the sets U_i are very small. The standard argument requires the sets M_0, M_1, M'_0, and M'_1 to be contained in U_4 and U_5 respectively.

   Since we start very close to a fixed point Π_4, the number k_1 required to reach the intersection of $u_1 \cap s'_1$ is rather large.

   Also, the following step, i.e., getting close to Π_i, results in large values of $k_2 - k_1$. There are two reasons for this: the sets U_i are very small and we want the transition map P^{k_2} defined on the appropriate subset of M_1 to fulfill the cone conditions, with respect to the expanding and contracting directions in U_4 and U_5. This is achieved by iterating P many times in U_5.
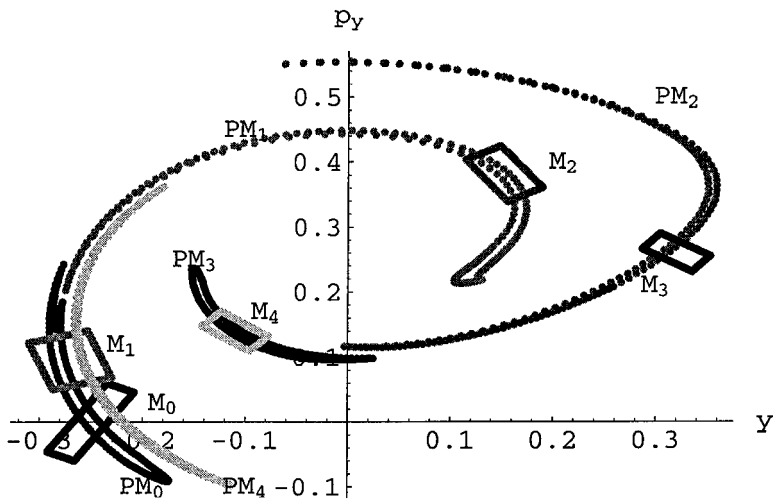
FIG. 2. The sets M_i and their images through P.

As a result of the standard argument we obtain a hyperbolic invariant set, but the dynamics on this set is very slow: most of the time the points stay close to the fixed points and from time to time they make sudden jumps to another fixed point.

3. THE POINCARÉ MAP

Let $\mathbb{T}$ be the triangle in the (x, y) plane with vertices $(0, 1)$, $(-\sqrt{3}/2, -1/2)$, and $(\sqrt{3}/2, -1/2)$; $\mathbb{T}$ is the closure of the bounded component of the so-called Hill region, i.e., the area where $V(x, y) < 1/6$ in the plane $(p_x = 0, p_y = 0)$, therefore the projection to the (x, y) plane of any motion starting on $\mathbb{T}$ cannot leave $\mathbb{T}$. Let $\mathbb{S} := \{(x, y, p_x, p_y) : H(x, y, p_x, p_y) = 1/6, (x, y) \in \mathbb{T}\}$.

Let $F_1 = (0, 1, 0, 0)$ and recall that the plane $(x = 0, p_x = 0)$ is invariant. The Hamiltonian restricted to this plane is

$$H(y, p_y) = 1/2(p_y^2 + y^2) - y^3/3,$$

and the point $(y, p_y) = (1, 0)$ corresponding to F_1 is a hyperbolic fixed point. It is easy to see that there exists a solution of the system homoclinic to F_1; indeed, the trajectories of the system are defined by the energy levels and on the energy level $E = 1/6$ we have the equation

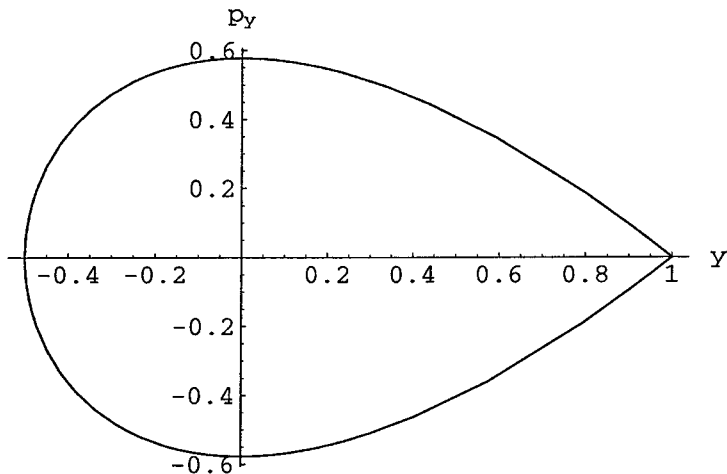$$1/2(p_y^2 + y^2) - y^3/3 = 1/6 \tag{3.1}$$

FIG. 3. Orbit homoclinic to $(1, 0)$ (and boundary of Ξ_1).

whose solutions in the half plane $(y \leqslant 1)$ are bounded and can be explicitly computed (see Fig. 3). We call Γ_1 the support of this homoclinic solution. By (3.1) we have

$$p_y = \pm \sqrt{\frac{1}{3} - y^2 + \frac{2y^3}{3}}, \tag{3.2}$$

which is the equation satisfied by points on Γ_1. Now consider the points $F_2 = R_-(F) = (-\sqrt{3}/2, -1/2, 0, 0)$ and $F_3 = R_+(F) = (\sqrt{3}/2, -1/2, 0, 0)$. By symmetry there exist solutions of the system $\Gamma_{2,3}$ at energy $1/6$ homoclinic to F_2 and F_3. We want to compute the intersections of such trajectories with Θ_1. Since for all points $(x, y, p_x, p_y) \in \Gamma_1$ we have $(x = 0, p_x = 0)$, then for such points

$$R_-(x, y, p_x, p_y)$$
$$= (-\sin(2\pi/3)\, y, \cos(2\pi/3)\, y, -\sin(2\pi/3)\, p_y, \cos(2\pi/3)\, p_y);$$

we want to compute the intersections of the set $\{R_-(x, y, p_x, p_y) : (x, y, p_x, p_y) \in \Gamma_1\}$ with the hyperplane $x = 0$ and $p_x > 0$, so we have $y = 0$ and $p_y < 0$, and by (3.2) we have $p_y = -1/\sqrt{3}$. A similar result holds for R_+, hence the intersections of Γ_2 and Γ_3 with Θ_1 are given by $(y, p_y) = (0, \pm\cos(2\pi/3)\, p_y) = (0, \pm 1/2\sqrt{3})$.

Lemma 2. *The trajectory of the system starting at every point $z \in \mathbb{S}$ which is not on Γ_i, $i = 1, 2, 3$, intersects the section $x = 0$, $p_x > 0$, infinitely many times (both for positive and negative time).*

Proof. We present the proof for positive times only, the proof for negative times is analogous.

Given a point $z = (x, y, p_x, p_y) \in \mathbb{R}^4$, by $z(t) = (x(t), y(t), p_x(t), p_y(t))$ we denote the image of the point z after time t.

The plane $A = \{(x, y, p_x, p_y) : p_x = 0, x = 0\}$ is invariant and all points in $\mathbb{S}$ which are not in Γ_1 do not intersect this plane. Hence we can use polar coordinates for the point (x, p_x). The angle $\alpha(t) = \alpha(x(t), p_x(t))$ is only defined mod 2π, so in order to have it well defined we may assume that $\alpha(0) \in [0, 2\pi)$. Furthermore we can compute $d\alpha/dt$ and the increase of the angle along the trajectory as a primitive of $d\alpha/dt$. We prove that either $\alpha(t)$ is unbounded or z is on $\Gamma_2 \cup \Gamma_3$. A direct computation shows that

$$\Omega(x(t), y(t), p_x(t), p_y(t)) := \frac{d\alpha}{dt} = -\frac{x^2(1 + 2y) + p_x^2}{x^2 + p_x^2}. \tag{3.3}$$

Since $y \geqslant -1/2$, then $d\alpha/dt \leqslant 0$.

Assume now that there exists $z \in \mathbb{R}^4$ such that the corresponding $\alpha = \alpha(t)$ is bounded. We prove that in this case either $z(t) \to F_2$ or $z(t) \to F_3$ as $t \to \infty$.

Assume that this is not the case. Consider an ω-limit set of z. Since the trajectory of z is contained in a compact set $\mathbb{S}$, the set $\omega(z)$ is nonempty, compact, connected, and invariant under the flow. We show that if $\omega(z)$ is not equal to $\{F_2\}$ or $\{F_3\}$, then it must contain a point q, such that

$$q \notin A, \qquad y(q) > -\tfrac{1}{2} \tag{3.4}$$

(by $x(q), y(q), p_x(q), p_y(q)$ we denote the x, y, p_x, p_y components of q respectively). First note that for all (x, y, p_x, p_y) in $\mathbb{S}$ we have

$$|\Omega(x, y, p_x, p_y)| < \varepsilon < 1 \qquad \text{iff} \quad y < -\frac{1}{2} + \frac{\varepsilon}{2} \quad \text{and} \quad x^2 > 0 \tag{3.5}$$

To see this note that $|\Omega| < \varepsilon < 1$ implies

$$x^2(1 + 2y) + p_x^2 < \varepsilon(x^2 + p_x^2),$$

so

$$x^2(1 + 2y) < x^2\varepsilon + p_x^2(\varepsilon - 1) < x^2\varepsilon.$$

From the above inequalities the condition (3.5) follows.

On the other hand, if $\varepsilon_1, \varepsilon_2 > 0$ are sufficiently small, $y(t) \leqslant -1/2 + \varepsilon_1/2$ and $|x(t)| \leqslant \sqrt{3}/2 - \varepsilon_2$, then $\dot{p}_y(t) \geqslant \delta > 0$. Since $\alpha(t)$ is bounded, then there exists a diverging sequence $\{t_n\}$ such that $|x(t_n)| \geqslant \sqrt{3}/2 - \varepsilon_2$. Now choose two vanishing sequences $\varepsilon_{1n}, \varepsilon_{2n}$ and extract subsequences to prove that

$(x(t_n), y(t_n)) \to (\pm \sqrt{3}/2, -1/2)$. Since we are on the energy level $1/6$ we also infer $(p_x(t_n), p_y(t_n)) \to (0, 0)$, i.e., either $(z(t_n)) \to F_2$ or $(z(t_n)) \to F_3$.

Without loss of generality we can assume that $F_2 \in \omega(z)$. Let q_1 be a point in $\omega(z)$ different from F_2. Since $\omega(z)$ is connected, then there exists a point $q_2 \in \omega(z)$ such that

$$0 < |x(q_2)| < \frac{\sqrt{3}}{2}.$$

If $y(q_2) > -\frac{1}{2}$, then set $q = q_2$. Otherwise, since $\dot{y} = p_y(q_2) = 0$ and $\dot{p}_y(q_2) > 0$, we can find a point q on the trajectory of q_2 with the desired properties. Since $\omega(z)$ is invariant under the flow, then $q \in \omega(z)$.

Observe that (3.4) implies that Ω is defined and continuous near q. Moreover,

$$\Omega(q) < 0.$$

Since $q \in \omega(z)$, then there exists a diverging sequence t_n and $\beta > 0$ such that $z(t_n) \to q$ and

$$\Omega(z(t)) < \frac{\Omega(q)}{2} < 0 \qquad \text{for all} \quad t \in \bigcup_{n=1}^{\infty} (t_n - \beta, t_n + \beta). \tag{3.6}$$

From (3.6) and (3.3) it follows that

$$\alpha(t_n + \beta) < n\beta\Omega(q).$$

Hence $\alpha(t)$ is unbounded, in contradiction to our assumption.

So far we have shown that if $\alpha(t)$ is bounded then $z(t)$ converges to either F_2 or F_3. It remains to show that if this is the case then z is on Γ_2 or Γ_3 respectively.

In order to establish the properties of the flow close to the points F_2 and F_3, we linearize the system at the symmetric point F_1 where the computations are simpler:

$$\dot{x} = p_x$$
$$\dot{y} = p_y$$
$$\dot{p}_x = -3x$$
$$\dot{p}_y = y.$$

The eigenvalues are $(\pm i\sqrt{3}, \pm 1)$ and the Hamiltonian is invariant with respect to the involution $(p_x, p_y) \to (-p_x, -p_y)$, hence by a theorem of Moser [M] (with a supplement of Rüssmann [R], see also [L]) there

exist symplectic coordinates (x_1, x_2, y_1, y_2) in which the Hamiltonian H has the form

$$H(x, y) = h_0(\xi, \eta) + \tfrac{1}{6}, \qquad \xi = x_1 y_1, \qquad \eta = (x_2^2 + y_2^2)/2,$$

where $h_0(\xi, \eta) = \lambda \xi + \omega \eta + o(\xi, \eta)$ and (x_1, x_2) are the momenta conjugated to the position variables (y_1, y_2), respectively. In our case $\omega = \sqrt{3}$, $\lambda = 1$. From this representation it follows that there can be at most two orbits converging to F_1 as $t \to \infty$ and only one of those is bounded. This implies that all trajectories converging to F_i, $i = 1, 2, 3$, have their support on Γ_i, and the proof of the lemma follows. ∎

Let $\Xi_1 \subset \Theta_1$ be the open set of points inside the curve $3(p_y^2 + y^2) - 2y^3 = 1$ (see Fig. 3) minus the points $(0, \pm 1/2\sqrt{3})$. Let Ξ_2 and Ξ_3 be the symmetric images of Ξ_1 with respect to R_- and R_+. Let $P_i: \Xi_i \to \Xi_i$ be the Poincaré maps and let $\tilde{P}_i: \Xi_i \to \Xi_{i+1}$ be the map defined by the flow (for simplicity let $\Xi_4 \equiv \Xi_1$).

LEMMA 3. *The maps P_i and $\tilde{P}_i$ are well defined.*

Proof. Choose a point $z \in \Xi_1$ and let $(x(t), y(t), p_x(t), p_y(t))$ be the solution of Eq. (1.2) with initial condition $(x(0), y(0), p_x(0), p_y(0)) = z$. By Lemma 2 the angle in the (x, p_x) plane $\alpha(t) := \alpha(x(t), p_x(t))$ is increasing and unbounded, therefore the trajectory of the system must intersect all sections Θ_i, $i = 1, 2, 3$, infinitely many times. By symmetry the same result holds for initial conditions on Ξ_2 and Ξ_3.

Remark 1. Observe that Lemma 3 holds also for all energies lower than $\tfrac{1}{6}$. The only modification is that in this case the Γ_i's are periodic orbits and we do not have to remove any points from the domains of P_i and $\tilde{P}_i$.

4. TOPOLOGICAL TOOLS

4.1. *General Definitions*

DEFINITION 1. A *triple set* (or *t-set*) is a triple $N = (|N|, N^l, N^r)$ of closed subsets of $\mathbb{R}^2$ satisfying the following properties

1. $|N|$ is a parallelogram, N^l and N^r are half-planes.

2. $N^l \cap N^r = \varnothing$

3. the sets $N^{le} := N^l \cap |N|$ and $N^{re} := N^r \cap |N|$ are two nonadjacent edges of $|N|$.

We call $|N|$, N^l, N^r, N^{le}, and N^{re} the support, the left side, the right side, the left edge, and the right edge of the t-set N, respectively.

Remark 2.   This definition of the triple set is in fact much more restrictive than needed: we can have any triple of sets homeomorphic to this definition. In fact we will need a triple set whose left and right sides are an intersection or union of two half-planes; see the definition of M_3 in the next section.

The usual picture of a triple set is given in Fig. 4.

Let $f: \mathbb{R}^2 \to \mathbb{R}^2$ be a map and let N_1 and N_2 be two triple sets.

DEFINITION 2.   We say that N_1 f-covers N_2 ($N_1 \overset{f}{\Rightarrow} N_2$) if

   a. $f(|N_1|) \subset \text{int}(N_2^l \cup |N_2| \cup N_2^r)$

   b.   either $f(N_1^{le}) \subset \text{int}(N_2^l)$ and $f(N_1^{re}) \subset \text{int}(N_2^r)$, or $f(N_1^{le}) \subset \text{int}(N_2^r)$ and $f(N_1^{re}) \subset \text{int}(N_2^l)$.

The following lemma says that we can reduce the condition (a) in the above definition to the boundary of $|N_1|$ if we know that the map f is injective.

LEMMA 4.   *Let* $f: \mathbb{R}^2 \to \mathbb{R}^2$ *be a map and let* N_1 *and* N_2 *be two triple sets. Assume that* f *is an injective map on* $|N_1|$, *then* $N_1 \overset{f}{\Rightarrow} N_2$ *if and only if*

   a′. $f(\partial \, |N_1|) \subset \text{int}(N_2^l \cup |N_2| \cup N_2^r)$

   b.   *either* $f(N_1^{le}) \subset \text{int}(N_2^l)$ *and* $f(N_1^{re}) \subset \text{int}(N_2^r)$ *or* $f(N_1^{le}) \subset \text{int}(N_2^r)$ *and* $f(N_1^{re}) \subset \text{int}(N_2^l)$.
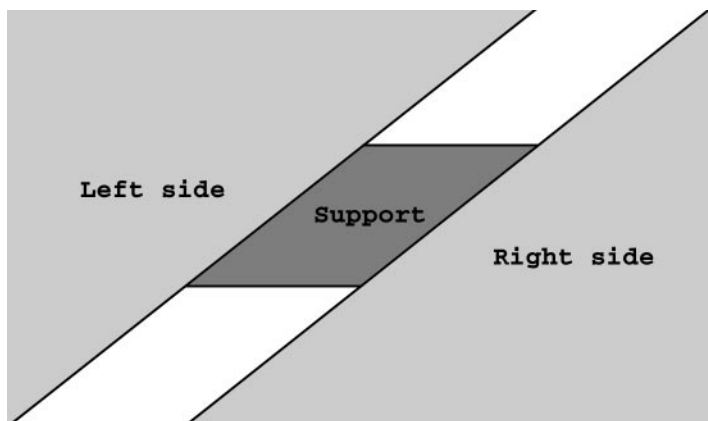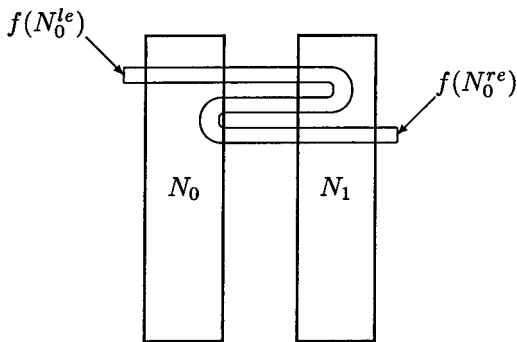

FIG. 4.   A triple set.

FIG. 5. An example of an f-covering relation: $N_0 \Rightarrow N_0, N_1$.

Proof. Condition [a] from Definition 2 follows easily from [a′] and the Jordan theorem (see [GZ, p. 180]). ∎

This lemma plays a very important role in the computer assisted verification of the covering relations, as it reduces the computations to the boundary of $|N_1|$ (see also Section 6 in [GZ] for more details).

Assume that we have n t-sets N_i, $i = 1, ..., n$, with some covering relations. Let $N = \bigcup_i |N_i|$; the following definitions are quite standard.

DEFINITION 3. Let f be injective. The invariant set of N is defined by $\mathrm{Inv}(N, f) := \{x \in N : f^i(x) \in N \text{ for all } i \in \mathbb{Z}\}$.

DEFINITION 4. The transition matrix $T(j, i)$, $i, j = 1, ..., n$, is defined as follows:

$$T(j, i) = \begin{cases} 1 & \text{if } N_i \stackrel{f}{\Rightarrow} N_j \\ 0 & \text{otherwise.} \end{cases}$$

The following theorem follows immediately from Theorem 4 in [Z3]:

THEOREM 1. *Given t-sets* $M_i \subset \mathbb{R}^2$ *and continuous maps* $f_i : M_i \to \mathbb{R}^2$, *such that*

$$M_0 \stackrel{f_0}{\Longrightarrow} M_1 \stackrel{f_1}{\Longrightarrow} M_2 \stackrel{f_2}{\Longrightarrow} M_2 \cdots \stackrel{f_{n-1}}{\Longrightarrow} M_0 = M_n,$$

then there exists $x \in \mathrm{int} |M_0|$, *such that* $f_k \circ \cdots \circ f_1 \circ f_0(x) \in \mathrm{int} |M_{k+1}|$, *for* $k = 0, ..., n-1$ *and* $x = f_{n-1} \circ \cdots \circ f_1 \circ f_0(x)$

Let Σ_n be the set of bi-infinite sequences of n symbols

DEFINITION 5. A sequence $\{x_n\} \in \Sigma_n$ is said to be admissible if $T(x_{n+1}, x_n) = 1$ for all n. We denote by $\Sigma_A \subset \Sigma_n$ the set of all admissible sequences.

DEFINITION 6. Assume $|N_i| \cap |N_j| = \varnothing$, for $i \neq j$. The projection π: Inv$(N, f) \to \Sigma_A$ is defined by setting $\pi(x)_i = j$ where j satisfies $f^i(x) \in |N_j|$ for all $i \in \mathbb{Z}$.

The set Σ_A inherits the topology from Σ_n; the shift map $\sigma: \Sigma_A \to \Sigma_A$ is continuous. We prove a semiconjugacy between σ and f, i.e., we prove that $\sigma \circ \pi = \pi \circ f|_{\text{Inv}(N, f)}$. In particular, this implies that there exists a symbolic dynamic structure on Inv(N, f).

The following theorem was proved in [Z3] (see Theorems 5 and 6) for the case $n = 2$. The following is a natural extension to a generic number of sets and the proof is exactly the same.

THEOREM 2. *The projection π is onto and if $\{x_n\} \in \Sigma_A$ is a periodic sequence, then $\pi^{-1}(\{x_n\})$ contain a periodic point.*

4.2. *Description of the Triple Sets*

All our triple sets (except M_3) will be defined by two pairs of parallel lines. The support is the area inside the lines, while the left (right) side is the area above the first line (below the second). In the following each couple of numbers (a, b) represents the line $p_y = ay + b$ in the plane (y, p_y).

M_0: $(1.819, 0.486)$, $(1.819, 0.424)$, $(-0.550, -0.206)$, $(-0.550, -0.069)$

M_1: $(0.325, 0.223)$, $(0.325, 0.143)$, $(-3.078, -0.833)$, $(-3.078, -0.639)$

M_2: $(0.635, 0.33)$, $(0.635, 0.24)$, $(-1.576, 0.584)$, $(-1.576, 0.659)$

M_3: $(-0.726, 0.511)$, $(-0.726, 0.474)$, $(1.376, -0.129)$, $(1.376, -0.231)$

M_4: $(1.209, 0.32)$, $(1.209, 0.226)$, $(-0.827, 0.068)$, $(-0.827, 0.03)$

N_0: $(1.819, 0.496)$, $(1.819, 0.413)$, $(-1.4, -0.41)$, $(-1.4, -0.318)$

N_1: $(0.325, 0.208)$, $(0.325, 0.134)$, $(-3.078, -0.862)$, $(-3.078, -0.701)$

$N_2 = M_2$

N_3: $(4.474, 1.22)$, $(4.474, 1.105)$, $(-0.224, -0.194)$, $(-0.224, -0.112)$

Figure 6 displays the supports of all sets and the invariant manifolds of Π_4 and Π_5. Note that (see Fig. 6)
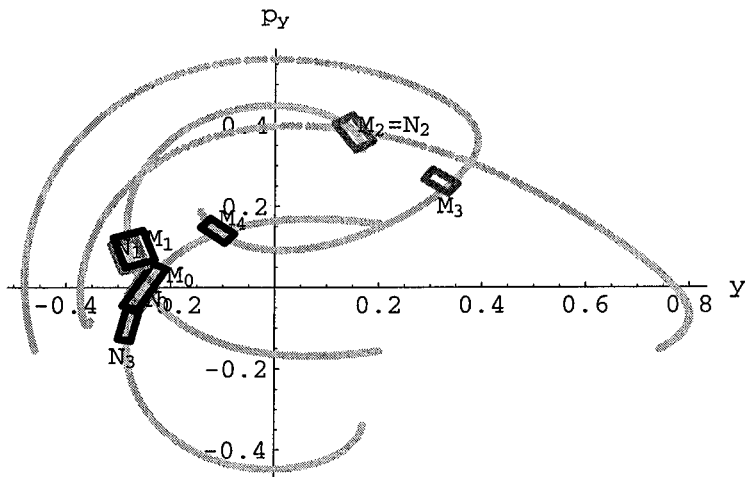
FIG. 6. The supports of all the triple sets used in the proof and the invariant manifolds.

$$|N_i| \cap |N_j| = \varnothing, \qquad i \neq j$$

$$|M_i| \cap |M_j| = \varnothing, \qquad i \neq j$$

$$|N_0| \cap |M_0| \neq \varnothing, \qquad |N_1| \cap |M_1| \neq \varnothing$$

$$|N_i| \cap |M_j| = \varnothing, \qquad (i, j) \notin \{(0, 0), (1, 1), (2, 2)\}. \qquad (4.1)$$

Although the support of M_3 is defined as the parallelogram enclosed in the lines given above as for the other sets, we could not choose half planes as its left and right side. The left side is instead the union of the half planes described by $p_y \geqslant -0.726y + 0.511$ and $p_y \geqslant 0.300$, while the right side is the intersection of the half planes described by $p_y \leqslant -0.726y + 0.474$ and $p_y \leqslant 0.290$.

We define $S_{ij}: \Theta_i \to \Theta_j$ by $S_{ij}(x, y, p_x, p_y) = R_-(x, y, p_x, p_y)$ if $(i, j) = (1, 2)$, $(i, j) = (2, 3)$, or $(i, j) = (3, 1)$; $S_{ij}(x, y, p_x, p_y) = R_+(x, y, p_x, p_y)$ if $(i, j) = (2, 1)$, $(i, j) = (3, 2)$, or $(i, j) = (1, 3)$; and $S_{ii} = identity$. Let $\Xi = \bigcup_i \Xi_i$.

With some abuse of notation which should not cause ambiguity we define the Poincaré map on $\bar{P}: \Xi \to \Xi$; more precisely,

$$\bar{P}(x) = \begin{cases} P_1(x) & \text{if } x \in \Xi_1, \\ P_2(x) & \text{if } x \in \Xi_2, \\ P_3(x) & \text{if } x \in \Xi_3. \end{cases}$$

We also define the "Poincaré map" between different sections $\tilde{P}: \varXi \to \varXi$ by

$$\tilde{P}(x) = \begin{cases} \tilde{P}_1(x) & \text{if } x \in \varXi_1, \\ \tilde{P}_2(x) & \text{if } x \in \varXi_2, \\ \tilde{P}_3(x) & \text{if } x \in \varXi_3. \end{cases}$$

Remark 3. It may seem that $\bar{P} = \tilde{P}^3$, but this is not necessarily true. It may happen e.g., that the trajectory of a point $z = (p_y, y)$ leaves the plane $\varXi_1$, hits $\varXi_2$ once, then hits $\varXi_3$ twice before coming back to the plane $\varXi_1$. In this case we have $\bar{P}(z) = P_1(z) = \tilde{P} \circ P_3 \circ \tilde{P} \circ \tilde{P}$. What happens is that the trajectory stays for some time very close to the plane $\varTheta_3$ (i.e., close to the homoclinic orbit) before going back to $\varTheta_1$. This is the actual behavior of the trajectory starting from $\varXi_1$ at $(y, p_y) = (-0.28, 0.1) \in |N_1|$; we think that it is possible to find points that after leaving $\varXi_1$ cut $\varXi_1$ and $\varXi_3$ as many times as we want before coming back to $\varXi_1$, provided they are sufficiently close to the homoclinic orbit.

Taking into account the symmetry, we have a total of 24 t-sets. Consider the ordered collection of t-sets $C_1 := (N_0, N_1, N_2, N_3, M_0, M_1, M_3, M_4)$ and let $C_i = S_{1i}(C_1)$ for $i = 2, 3$. Let O be an ordered collection built as a concatenation of C_1, C_2, and C_3; let $P: \bigcup_{i=1}^{24} |O_i| \to \varXi$ be defined by

$$P(x) := \begin{cases} \tilde{P}(x) & \text{if } x \in |N_2| \cup S_{12}(|N_2|) \cup S_{13}(|N_2|) \\ \bar{P}(x) & \text{otherwise.} \end{cases}$$
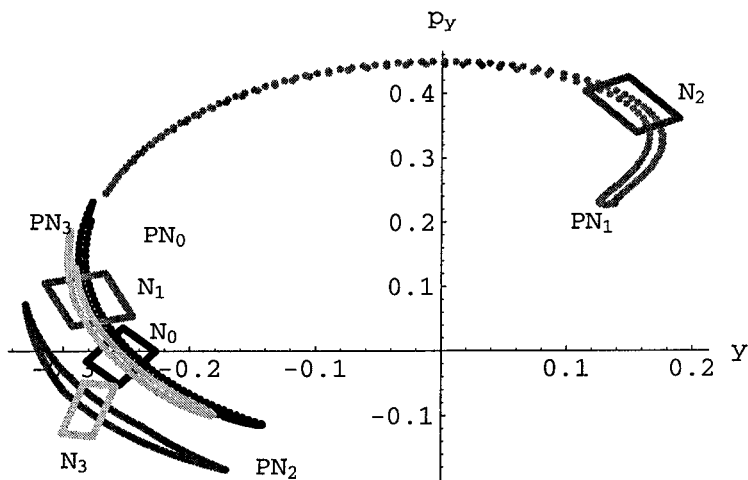

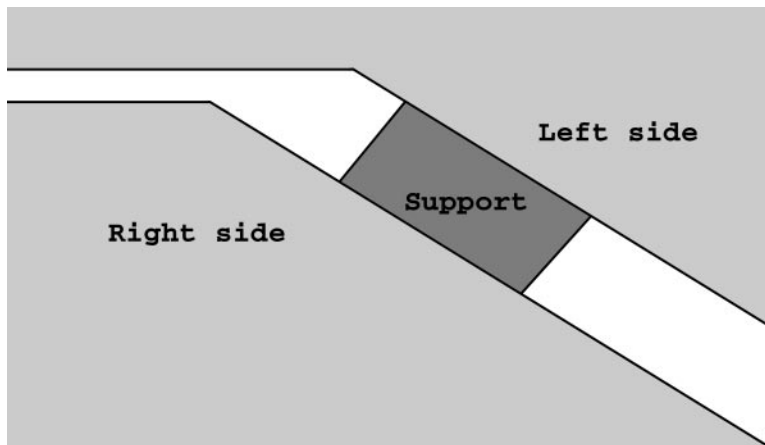**FIG. 7.** The sets N_i and their images through P.

FIG. 8.   The triple set M_3.

5. MAIN RESULTS

We denote by $\Rightarrow$ the covering with respect to the map P. The following lemma was proved with computer assistance.

LEMMA 5.   *The following covering relations hold.*

$$M_0 \Rightarrow M_0 \Rightarrow M_1 \Rightarrow M_2 \Rightarrow M_3 \Rightarrow M_4 \Rightarrow \begin{matrix} M_0 \\ M_1 \end{matrix}, \tag{5.1}$$

$$N_0 \Rightarrow N_0 \Rightarrow N_1 \Rightarrow N_2 \Rightarrow S_{12}(N_3), \tag{5.2}$$

$$N_3 \Rightarrow \begin{matrix} N_0 \\ N_1 \end{matrix}, \tag{5.3}$$

$$M_0 \Rightarrow N_0 \qquad and \qquad N_0 \overset{\mathrm{id}}{\Longrightarrow} M_0. \tag{5.4}$$

Details concerning the rigorous computer assisted proof of Lemma 5.1 are contained in Section 6.

Remark 4.   In order to achieve a simpler description of the t-sets involved in the computations, we prefer to restrict our attention to the plane (y, p_y). For example to illustrate and to prove the covering relation $N_2 \overset{\tilde{P}}{\Rightarrow} S_{12}(N_3)$, we will instead consider the covering relation $N_2 \overset{S_{21} \circ \tilde{P}}{\Longrightarrow} N_3$, which is equivalent. To see this, as an example assume we want to check the first of properties (b) of $N_2 \overset{\tilde{P}}{\Rightarrow} S_{12}(N_3)$, i.e. we have to check that the left edge of N_2 is mapped by $\tilde{P}$ to the left side of $S_{12}(N_3)$. By definition of

$S_{12}(N_3)$, this is equivalent to showing that $\tilde{P}(N_2^l) \subset \text{int}(S_{12}(N_3^l))$, which can be written as $S_{21} \circ \tilde{P}(N_2^l) \subset \text{int}(N_3^l)$, that is the same property of $N_2 \xrightarrow{S_{21} \circ \tilde{P}} N_3$.

Remark 5. We have used Lemma 4 to verify the covering relations. By continuity arguments it follows that Lemma 5 also holds for energy values in the interval $(\frac{1}{6} - \delta, \frac{1}{6} + \delta)$, for some small $\delta > 0$.

Remark 6. The length of the computer assisted proof of Lemma 3 is kept to a minimum by Lemma 5 which guarantees that the map P is well defined and injective. Indeed, without such a lemma, we would have to check that the map is well defined by a rigorous numerical procedure in the whole part of Θ_1 covered by the t-sets.

Observe that from Lemma 5 we immediately have the following.

COROLLARY 1.

$$N_3 \Rightarrow M_0 \tag{5.5}$$

By symmetry, the same covering relations occur if we apply the map S_{12} or S_{13} to all covering relations in Lemma 5.

Let T be a transition matrix induced by the chains of covering relations from Lemma 5 and their symmetric images on O_i for $i = 1, 2, ..., 24$.

Observe that we cannot apply Theorem 2 to the map P and the matrix T, because the supports of the sets O_i are not disjoint (see (4.1)). However, from Theorem 1 we obtain the following.

THEOREM 3. *For every $\{i_n\} \in \Sigma_T$ there exists $x \in \Xi$, such that*

$$P^n(x) \in |O_{i_n}|, \qquad n \in \mathbb{Z},$$

and if $\{i_n\}$ is periodic, then x is a periodic point for P with the same principal period.

The above theorem is the most general statement of our results. Since the matrix T is huge, with plenty of zeros, we will also present and discuss a few less general consequences of Lemma 5.

COROLLARY 2. *There exists $x_1 \in N_0$ such that $P_1(x_1) = x_1$. Moreover, by symmetry the points $S_{1i}(x_1) \in S_{1i}(N_0)$ are fixed points for the maps P_i, $i = 2, 3$.*

Proof. The existence of x follows from the covering relation

$$N_0 \overset{P}{\Rightarrow} N_0$$

and the fact that $P_1 = P$ on N_0. ∎

The fixed point for P_1, whose existence is established in the above corollary, can be identified with the point Π_4 from [CPR]. However, we cannot claim this for sure, because we did not prove that $p_y(x_1) = 0$, as is the case for Π_4.

The following two corollaries establish the existence of the symbolic dynamics on two symbols (a horseshoe dynamics)

COROLLARY 3.   *The map* π: $\mathrm{Inv}(|M_0| \cup |M_1|, P_1^5) \to \{0, 1\}^{\mathbb{Z}}$ *given by the condition* $\pi(x)_i = j$ *if and only if* $P_1^{5i}(x) \in |M_j|$, *is onto. If* $\alpha \in \{0, 1\}^{\mathbb{Z}}$ *is periodic with period* l, *then* $\pi^{-1}(\alpha)$ *contains a point of period* l *for the map* P_1^5.

Proof. Observe that on M_i for $i = 0, 1, ..., 4$ we have $P = P_1$. The existence of symbolic dynamics on two symbols follows now directly from (5.1) and Theorem 1. ∎

COROLLARY 4.   *The map* π: $\mathrm{Inv}(|N_0| \cup |N_1|, P^8) \to \{0, 1\}^{\mathbb{Z}}$, *given by the condition* $\pi(x)_i = j$ *if and only if* $P^{8i}(x) \in |N_j|$, *is onto. If* $\alpha \in \{0, 1\}^{\mathbb{Z}}$ *is periodic with the period* l, *then* $\pi^{-1}(\alpha)$ *contains a point of period* l *for the map* P^8.

Proof. Observe that from (5.2) and (5.3) it follows that we have the following chain of covering relations

$$N_1 \Rightarrow N_2 \Rightarrow S_{12}(N_3) \Rightarrow S_{12}(N_1) \Rightarrow S_{12}(N_2)$$
$$\Rightarrow S_{13}(N_3) \Rightarrow S_{13}(N_1) \Rightarrow S_{13}(N_2) \Rightarrow N_0, N_1 .$$

The above chain has length 8. It is easy to build chains of covering relations of the same length which begin with N_0 and end with N_0 and N_1 as follows

$$N_0 \Rightarrow N_0 \Rightarrow \cdots \Rightarrow N_0, N_1.$$

We now apply Theorem 1 to get the result. ∎

Remark 7.   By combining in different ways the covering relations and the symmetries we can obtain a rich dynamics for the system; e.g., we can consider the chain from N_0 to $S_{12}(N_0)$, then to $S_{12}(M_0)$, and back to $S_{12}(M_0)$ through all the sets $S_{12}(M_i)$, then again to $S_{12}(N_0)$ and back to N_0 through (5.2) twice, etc.

COROLLARY 5.   *The map P_1 has periodic point of period n for every $n \geqslant 4$.*

Proof.   We look for periodic points in the sets $|M_i|$. On those sets we have $P_1 = P$, hence it is enough to prove the assertion for the map P.

By Theorem 1 it is enough to prove the existence of a chain of covering relations of length n, for $n \geqslant 4$. To guarantee that the period of the obtained periodic point is equal to n, we have to build these chains in a way which excludes smaller periods.

A periodic point of period 4 is obtained from the following chain of covering relations:

$$M_1 \Rightarrow M_2 \Rightarrow M_3 \Rightarrow M_4 \Rightarrow M_1.$$

For $n > 4$ we consider the chain of covering relations built from the chain

$$M_0 \Rightarrow M_1 \Rightarrow M_2 \Rightarrow M_3 \Rightarrow M_4 \Rightarrow M_0$$

and supplemented by the chain built of $n - 5$ covering relations $M_0 \Rightarrow M_0$.   ∎

Figure 9 represents all the triple sets in Θ_1 plus the images of all their symmetric sets on Θ_2 and Θ_3 under the maps P_{21} and P_{31}. More precisely, in Fig. 9 we see the supports of all the triple sets M_i and N_i described above and their images under $P_{12} \circ S_{21}$ and $P_{13} \circ S_{31}$, i.e., the area where the chaotic motion takes place.
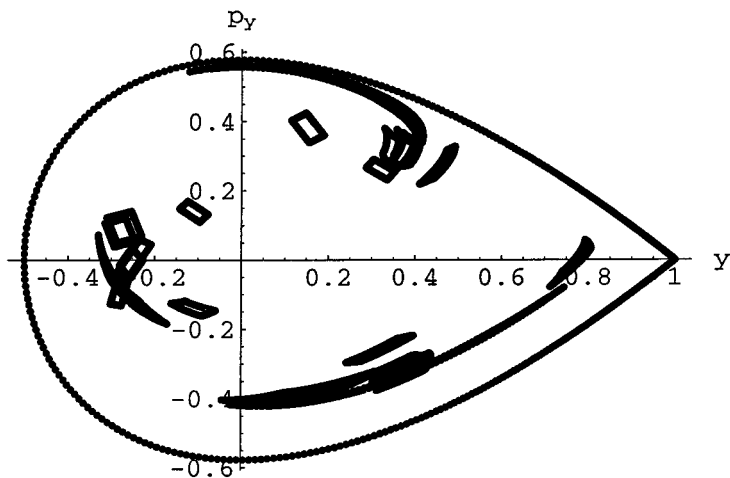

FIG. 9.   All sets M_i, N_i and their images through $P_{12} \circ S_{21}$ and $P_{13} \circ S_{31}$.

5.1. *Topological Entropy Estimates*

For a map f let $h_t(f)$ denote the topological entropy of a map f (see [W]). We want to estimate the topological entropy of the map P_1. To this purpose we use the following lemma:

LEMMA 6. *Let $f: X \to X$ be a continuous map. Let $S \subset X$ be an invariant set, and let A be an $n \times n$ matrix such that there exists a surjective map $\pi: S \to \Sigma_A$ satisfying $\sigma \circ \pi = \pi \circ f$. Then $h_t(f) \geqslant \ln(\max\{|\lambda_i|, \lambda_i$ is an eigenvalue of $A\}$.*

Proof. The proof is an easy consequence of Theorem 7.13 in [W] and is left to the reader. ∎

We do not know what the relation is between iterations of P and P_1 (see Remark 3), therefore we base our computation of the topological entropy for P_1 on (5.1) only.

COROLLARY 6. $h_t(P_1) > 1.38$.

Proof. Consider the collection of t-sets $(M_0, M_1, M_2, M_3, M_4)$. Let A be the transition matrix resulting from the chain (5.1): We have

$$A = \begin{bmatrix} 1 & 0 & 0 & 0 & 1 \\ 1 & 0 & 0 & 0 & 1 \\ 0 & 1 & 0 & 0 & 0 \\ 0 & 0 & 1 & 0 & 0 \\ 0 & 0 & 0 & 1 & 0 \end{bmatrix}.$$

By Lemma 6 a lower bound for h_t is given by the maximal norm eigenvalue of the matrix A. The characteristic polynomial is $p(x) = -x(x^4 - x^3 - 1)$, and since $p(1.38027) = 5.018 \times 10^{-5}$ and $p(1.38028) = -1.6116 \times 10^{-5}$, then $h_t(P_1) > 1.38027$. ∎

5.2. *Other Energy Levels*

Since by Remark 5 Lemma 5 holds also for all energies $E \in (\frac{1}{6} - \delta, \frac{1}{6} + \delta)$ for some small $\delta > 0$, we can infer that all the results in this section are valid for this energy range.

6. RIGOROUS NUMERICS FOR ODE'S

In this section we describe the essential points of the rigorous numerics we used to solve our problem. We describe briefly the main problem one

faces when doing rigorous numerics, the *wrapping effect*, and the Lohner Algorithm we used to contain it. We decided to include here a short description of the Lohner Algorithm, because it appears to be unknown outside the interval arithmetic community.

Some details like how we produce the Poincaré map from computed rigorous enclosures of trajectories or how we check our covering relations are rather obvious, so we do not include them here.

6.1. *Interval Arithmetic*

We performed our computations using interval arithmetic. This means that instead of dealing with real numbers, we have done all operations on intervals to include round–off errors (see [MM3] and the references cited there for more details about this topic).

In the following, by letters we denote single-valued objects like vectors, real numbers, and matrices. By square brackets we denote sets, for example, $[f(x + [r])] := \{y : | : y = f(x + t), : t \in [r]\}$. By angular brackets $\langle \cdot \rangle$ we denote the computer realization of the operation inside these brackets using interval arithmetic. For example, $x \langle + \rangle y$ represents an interval which contains $x + y$. For a function F, by $\langle F \rangle$ we denote its computer realization obtained by replacing every ideal operation with its computer realization. For a set $[r]$, by $\langle r \rangle$ we denote its interval hull realized by the computer (this means the smallest product of intervals which is representable by the computer and contains the set $[r]$). We have

$$\Phi(x) \in \langle \Phi(x) \rangle, \qquad [\Phi([r])] \subset \langle \Phi(\langle r \rangle) \rangle.$$

6.2. *Wrapping Effect*

The main problem one faces when trying to do rigorous numerics for ordinary differential equations is the *wrapping effect*.

Let

$$R_\alpha = \begin{bmatrix} \cos(\alpha) & -\sin(\alpha) \\ \sin(\alpha) & \cos(\alpha) \end{bmatrix}, \qquad [x] = [-\delta, \delta]^2$$

Consider now the evaluation in interval arithmetic of the product $R_\alpha[x]$. For $|\alpha| < \pi/2$ the result is

$$R_\alpha \langle \cdot \rangle [x] \supset (\cos(\alpha) + |\sin(\alpha)|)[-\delta, \delta]^2.$$

Hence for a map which is an isometry we see that its computer realization has a growth factor $\cos(\alpha) + |\sin(\alpha)| > 1$ for $\alpha \neq 0$.

Observe that when solving the system of equations of the harmonic oscillator

$$\dot{x} = -y, \qquad \dot{y} = x, \tag{6.1}$$

the 2π-shift along the trajectory for (6.1) is an identity map, but when we compute it numerically in interval arithmetic we have to compose a map R_h, where h is the time step used in the numerical scheme. An easy computation shows that for the 2π map for this system we obtain a growth factor $e^{2\pi} \approx 535$ as $h \to 0$.

For more complicated equations like the Lorenz system, the effect is even worse (see [GZ]).

6.3. *Lohner Algorithm*

We describe briefly the version of the Lohner Algorithm [Lo] we used in our computations.

Consider the ordinary differential equation

$$x' = f(x), \qquad x \in \mathbb{R}^n, \tag{6.2}$$

inducing a dynamical system which we denote by φ.

Let $\Phi(h, x)$ be a Taylor method for solving Eq. (6.2), where $h \in \mathbb{R}$ and $x \in \mathbb{R}^n$. We have

$$\varphi(h, x) \in \Phi(h, x) + [w], \tag{6.3}$$

where $[w]$ is the remainder term calculated over the set containing $\varphi([0, h], x)$.

Our aim is to estimate $[\varphi(h, x_k + [r_k])]$, where x_k is a vector and $[r_k]$ is a set. One of the basic ideas of Lohner is to use the Jacobian matrix for the explicitly known function $\Phi(h, \cdot)$ instead of trying to estimate the Jacobian matrix for $\varphi(h, \cdot)$.

We proceed as follows:

Step 1. We find a rough enclosure D for $[\varphi([0, h], x_k + [r_k])]$ (we choose $D = \Xi_1$).

Step 2. We calculate the error term appearing in (6.3), $[w] := [w](D)$ on D, by evaluating $x^{(r+1)}$ on D using the formulas for the time derivatives of the solutions, which are easy to compute in this case.

Step 3. From (6.3) we have

$$[\varphi(h, x_k + [r_k])] \subset [\Phi(h, x_k + [r_k])] + [w].$$

Consider $\Delta x \in [r_k]$. We apply the Lagrange mean value theorem to $\Phi_i(h, x_k + \Delta x)$ to obtain

$$\Phi_i(h, x_k + \Delta x) = \Phi_i(h, x_k) + \sum_{i=1}^{n} \frac{\partial \Phi_i(h, x_k + \theta \Delta x)}{\partial x_j} \Delta x_j$$

for every $i = 1, ..., n$, $\Delta x \in [r_k]$ and $\theta = \theta(i, \Delta x) \in [0, 1]$.

Let us denote by $[A_k]$ an array whose entries are given by

$$[A_{k, ij}] := \left[\frac{\partial \Phi_i(h, x_k + [r_k])}{\partial x_j} \right].$$

Since $\Delta x \in [r_k]$ we obtain

$$[\varphi(h, x_k + [r_k])] \subset \Phi(h, x_k) + [A_k] \cdot [r_k] + [w]. \tag{6.4}$$

Step 4. Let

$$x_{k+1} = \text{the middle point of } (\langle \Phi(h, x_k) \rangle + [w]),$$

$$[z_{k+1}] = (\langle \Phi(h, x_k) \rangle + [w]) - x_{k+1},$$

$$[r_{k+1}] = [A_k][r_k] + [z_{k+1}].$$

From (6.4) it follows easily that

$$[\varphi(h, x_k + [r_k])] \subset x_{k+1} + [r_{k+1}].$$

Iterating this procedure, we obtain

$$[\varphi(nh, x_0 + [r_0])] \subset x_n + [r_n]$$

where

$$[r_{k+1}] = [A_k][r_k] + [z_{k+1}].$$

Let us remark that in the above discussion we used ideal mathematical arithmetic operations, but in numerical calculations we have to prevent the wrapping effect. Therefore we have to find an efficient algorithm to evaluate the recursively defined sequence of $[r_k]$. More precisely we need to avoid the multiplication $[A_k][r_k]$, which is the source of the wrapping effect.

We used the method which Lohner calls *inner enclosure*, which is devised for the situation when the initial size of $[r_0]$ is large when compared with other errors (round-off errors and the rest term in the Taylor method).

In this approach we never compute $[r_{k+1}]$ explicitly, but we use an additional variable $[\tilde{r}_{k+1}]$ recursively defined by setting $[\tilde{r}_0] = \{0.0\}^n$ and $[\tilde{r}_{k+1}] = [A_k][\tilde{r}_k] + [z_{k+1}] + ([A_k] C_k - C_{k+1})[r_0]$, where $C_0 := I$ and

C_{k+1} is a middle point of $[A_k]C_k$. By these definitions we have $[r_{k+1}] = C_{k+1}[r_0] + [\tilde{r}_{k+1}]$, and due to the splitting of r_k into $C_k[r_0]$ and $[\tilde{r}_k]$, the wrapping effect is present only in the term $[\tilde{r}_k]$, which is in our computations much smaller than the other one arising from $[r_0]$.

6.4. *Some Technical Data Concerning the Computations*

We use the Lohner Algorithm with a third-order Taylor method. The time step is for most edges $h = 0.05$, but for a few edges we need $h = 0.025$. The edges are divided into 100–300 segments, depending on the edge. The Poincaré return times are in this range [6, 10].

We used a computer running the Linux O.S. equipped with a 450-MHz Pentium III CPU. The total computation time was approximately 2 hours and 40 minutes. The interval arithmetic and Lohner Algorithm were implemented in $C++$ and compiled using the *gnu* compiler.

REFERENCES

[BGM]   J. C. Bastos de Figueiredo, C. Grotta Ragazzo, and C. P. Malta, Two important numbers in the Hénon–Heiles dynamics, *Phys. Lett. A* **241** (1998), 35–40.

[CKR]   R. C. Churchill, M. Kummer, and D. L. Rod, On averaging, reduction, and symmetry in Hamiltonian systems, *J. Differential Equations* **49** (1983), 359–414.

[CPR]   R. C. Churchill, G. Pecelli, and D. L. Rod, "A Survey of the Hénon–Heiles Hamiltonian with Applications to Related Examples," Lecture Notes in Physics, Vol. 93, pp. 76–136, Springer-Verlag, New York/Berlin, 1978.

[CPRI] R. C. Churchill, G. Pecelli, and D. L. Rod, Stability transitions for periodic orbits in hamiltonian systems, *Arch. Rational Mech. Anal.* **73** (1980), 313–347.

[CRI]   R. C. Churchill and D. L. Rod, Pathology in dynamical systems. I. General theory, *J. Differential Equations* **21** (1976), 39–65.

[CRII] R. C. Churchill and D. L. Rod, Pathology in Dynamical Systems. II. Applications, *J. Differential Equations* **21** (1976), 66–112.

[CRIII] R. C. Churchill and D. L. Rod, Pathology in Dynamical Systems. III. Analytic Hamiltonians, *J. Differential Equations* **37** (1980), 23–38.

[CRIV] R. C. Churchill and D. L. Rod, Homoclinic and heteroclinic orbits of reversible vectorfields under perturbation, *Proc. Roy. Soc. Edinburgh Ser. A* **102** (1986), 345–363.

[E]   R. Easton, Isolating blocks and symbolic dynamics, *J. Differential Equations* **17** (1975), 96–118.

[GH]   J. Guckenheimer and P. Holmes, "Nonlinear Oscillations, Dynamical Systems, and Bifurcations of Vector Fields," Springer-Verlag, New York/Heidelberg/Berlin.

[GZ]   Z. Galias and P. Zgliczyński, Computer assisted proof of chaos in the Lorenz system, *Physica D* **115** (1998), 165–188.

[GR1]   C. Grotta Ragazzo, Nonintegrability of some Hamiltonian systems, scattering and analytic continuation, *Comm. Math. Phys.* **166** (1994), 255–277.

[GR2]   C. Grotta Ragazzo, Irregular dynamics and Homoclinic orbits to Hamiltonian saddle-centers, *Comm. Pure Appl. Math.* **50** (1997), 105–147.

[HH]   M. Hénon and C. Heiles, The applicability of the third integral of motion, *Astron. J.* **69** (1964), 449–457.

[HZHT] B. Hassard, J. Zhang, S. Hastings, and W. Troy, A computer proof that the Lorenz equations have "chaotic" solutions, *Appl. Math. Lett.* **7** (1994), 79–83.

[L]   L. M. Lerman, Hamiltonian systems with loops of a separatrix of a saddle-center, *Sel. Math. Sov.* **10**, No. 3 (1991), 297–306.

[Lo]   R. J. Lohner, Computation of guaranteed enclosures for the solutions of ordinary initial and boundary value problems, *in* "Computational Ordinary Differential Equations" (J. R. Cash and I. Gladwell, Eds.), Clarendon Press, Oxford, 1992.

[LF]   G. H. Lunsford and J. Ford, On the stability of periodic orbits for nonlinear oscillator systems in regions exhibiting stochastic behavior, *J. Math. Phys.* **13** (1972), 700–705.

[MHO]   A. Mielke, P. Holmes, and O. O'Reilly, Cascades of homoclinic orbits to, and chaos near, a Hamiltonian saddle-center, *J. Dynam. Differential Equations* **4**, No. 1 (1992), 95–126.

[MM1]   K. Mischaikow and M. Mrozek, Isolating neighbourhoods and chaos, *Japan J. Indust. Appl. Math.* **12** (1995), 205–236.

[MM2]   K. Mischaikow and M. Mrozek, Chaos in the Lorenz equations: A computer assisted proof, *Bull. Amer. Math. Soc.* **32** (1995), 66–72.

[MM3]   K. Mischaikow and M. Mrozek, Chaos in the Lorenz equations: A computer assisted proof. II: Details, *Math. Comput.* **67** (1998), 1023–1046.

[M]   J. Moser, On the generalization of a theorem of Liapunov, *Comm Pure Appl. Math.* **11** (1958), 257–271.

[MC]   J. J. Morales-Ruiz and C. Simo, Non-integrability criteria for Hamiltonians in the case of lamé normal variational equations, *J. Differential Equations* **129** (1996), 111–135.

[MP]   J. J. Morales-Ruiz and J. P. Peris, On a Galosian approach to the splitting of separatrices, *Ann. Faculté Sci. Toulouse* **8** (1999), 125–141.

[NR]   A. Neumaier and T. Rage, Rigorous chaos verification in discrete dynamical systems, *Physica D* **67** (1993), 327–346.

[RNS]   T. Rage, A. Neumaier, and C. Schlier, Rigorous verification of chaos in a molecular model, *Phys. Rev. E* **50** (1994), 2682–2688.

[R]   H. Rüssmann, Über das Verhalten analitischer Hamiltonscher Differential-Gleichungen in der Nähe einer Gleichgewichtlösung, *Math. Ann.* **154**, No. 4 (1964), 285–300.

[T]   W. Tucker, Lorenz attractor exists, preprint.

[W]   P. Walters, "An Introduction to Ergodic Theory," Springer-Verlag, New York, 1982.

[Z1]   P. Zgliczyński, Fixed point index for iterations, topological horseshoe and chaos, *Topol. Methods Nonlinear Anal.* **8**, No. 1 (1996), 169–177.

[Z2]   P. Zgliczyński, Computer assisted proof of chaos in the Hénon map and in the Rössler equations, *Nonlinearity* **10**, No. 1 (1997), 243–252.

[Z3]   P. Zgliczyński, Sharkovskii′s Theorem for multidimensional perturbations of 1-dim maps, *Ergodic Theory Dynam. Systems* **19** (1999), 1655–1684.